Proton Localization in an Asymmetric Double-Minimum Potential: 2-Methyl-9-hydroxyphenalenone

R. Rossetti, R. Rayford,† R. C. Haddon, and L. E. Brus*

Contribution from Bell Laboratories, Murray Hill, New Jersey 07974.
Received November 20, 1980

Abstract: Vibronically resolved electronic spectroscopy in low-temperature neon and argon matrices has been used to determine the shape of the asymmetric double-minimum potential-energy curve in both ground and excited electronic states of the title compound. The theory and experimental analysis of vibronic tunneling mode transitions are discussed in the limits of both common asymmetry and reversed asymmetry. Methyl substitution in the 2 position of 9-hydroxyphenalenone induces an asymmetry in the potential minima of the ground state of $\Delta E \simeq 180\ cm^{-1}$. The asymmetry is sufficient to substantially localize the vibrational wave function in the ground electronic state, but not in the excited electronic state.

Recently we reported a matrix isolation spectroscopic study (hereafter referred to as I) of proton tunneling in the ground and lowest excited singlet state of 9-hydroxyphenalenone (**1**).[1] Equivalent molecular structures arise as the phenolic proton transfers between the two oxygens, producing a symmetric double-minimum potential curve as shown in Figure 1. We determined the shape of this potential in both electronic states, using an approximate theoretical model with our spectroscopic and other X-ray structural data. In the ground state, **1**-*h* and **1**-*d* tunnel on the ~0.13 ps and ~1.7 ps time scales, respectively. The barrier to tunneling is substantially lower in the excited state.

We now investigate the effect that asymmetric substitution has on the equilibrium structure and tunneling dynamics. Are the dynamics principally sensitive only to local interactions near the O···H···O chelate group, or can the rates be strongly influenced by π-electron perturbations at some distance? **1** provides an interesting test molecule because, starting with the symmetric parent, one can study either "weak" or "strong" perturbations occuring either "near" or "far" from the chelate group. For example, **2** in Chart I represents a weak, relatively near perturbation while **3** represents a more drastic perturbation of the π-electronic structure. How asymmetric are the potentials in **2** and **3**, and to what extent is the proton localized on one oxygen?

Derivatives in which the two oxygens are strongly inequivalent are similar to other internally hydrogen bonded molecules such as methyl salicylate (**4**), salicylideneaniline (**5**), and 2-(2-hydroxyphenyl)benzothiazole (**6**). In the ground state of **4** there is a strong hydrogen bond to the carboxylic oxygen, but no evidence for a second local minimum near this oxygen.[2] In the first excited electronic state, however, the carboxylic oxygen provides the stable local minimum for the proton, and the proton transfers within a few picoseconds, even at 4 K, following Franck–Condon (vertical) electronic excitation.[3] In the excited state there is no evidence for a second minimum on the original (phenolic) oxygen. In the scheme of Figure 1, **4** is an extreme example of reverse asymmetry. Similar phenomena occur in **5** and **6** as shown by their picosecond fluorescence kinetics.[4,5]

In this paper we apply the technique of vibronically resolved electronic spectroscopy to determine the asymmetric potential shape and vibrational localization in **2**, which can be formulated as either 2-methyl-9-hydroxyphenalenone (shown) or 8-methyl-9-hydroxyphenalenone. As this is, to our knowledge, the first time even an approximate experimental analysis of this type has been performed, we discuss the spectral structure in some detail.

Experimental Section

The apparatus and techniques are substantially unchanged from I. Briefly, we observe spectrally resolved fluorescence from matrix-isolated samples of **2**[6] following tunable dye laser excitation near 430 nm. The excitation and emission spectra are normalized to the dye laser power.

† Bell Laboratories Undergraduate Research Student.

Chart I

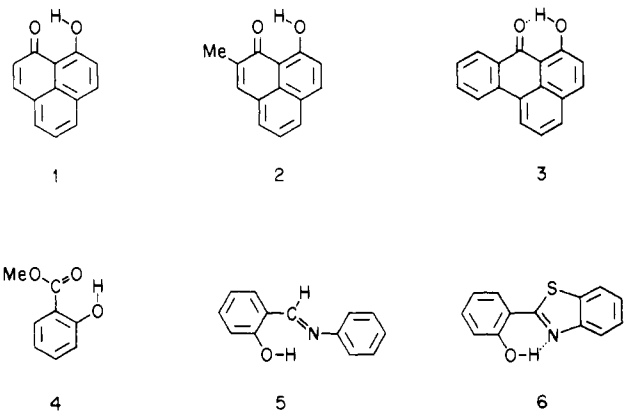

1 2 3 4 5 6

A gaseous mixture of the compound in flowing Ne or Ar is made by entrainment of the sublimated vapor, and subsequently deposited on a cold Pt substrate.

Observations and Discussion

A. Tunneling Transitions. In a symmetric double-minimum potential the lowest $v = 0$ level is split into two components O^+ and O^- via the tunneling between the two wells. The isotopically dependent splitting Δ between O^+ and O^- is related to the tunneling time τ via $\tau = h/2\Delta$. If ψ_1 and ψ_2 are taken to be localized vibrational basis wave functions in the two wells, then the O^+ and O^- delocalized molecular wave functions are

$$\phi^{\pm} = \psi_1 \pm \psi_2 \qquad (1)$$

In an allowed electronic transition between two such states, the quantum mechanical Franck–Condon principle indicates that only the $O^+ \rightarrow O^+$ and $O^- \rightarrow O^-$ vibronic components can occur if the potential is symmetric. In absorption, the $O^+ \rightarrow O^+$ line originates on the true vibronic ground state O^+. The $O^- \rightarrow O^-$ component only appears as the temperature is raised to the point that the O^- component becomes thermally populated. In **1**-*d* we found the temperature-dependent $O^- \rightarrow O^-$ line, and from its Arrhenius be-

(1) R. Rossetti, R. C. Haddon, and L. E. Brus, *J. Am. Chem. Soc.*, **102**, 6913 (1980).
(2) J. Goodman and L. E. Brus, *J. Am. Chem. Soc.*, **100**, 7472 (1978).
(3) K. K. Smith and K. J. Kaufman, *J. Phys. Chem.*, **82**, 2286 (1978).
(4) P. F. Barbara, P. M. Rentzepis, and L. E. Brus, *J. Am. Chem. Soc.*, **102**, 2786 (1980).
(5) P. F. Barbara, L. E. Brus, and P. M. Rentzepis, *J. Am. Chem. Soc.*, **102**, 5631 (1980).
(6) R. C. Haddon, R. Rayford, and A. M. Hirani, *J. Org. Chem.*, submitted.

0002-7863/81/1503-4303$01.25/0

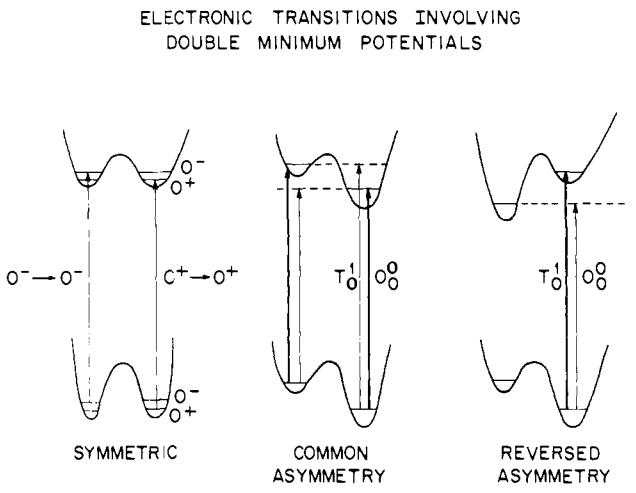

Figure 1. Schematic diagram of vibronic transitions involving double-minimum potential-energy curves. In the left-hand case of a symmetric potential, only the $O^+ \rightarrow O^+$ and $O^- \rightarrow O^-$ vibronic components occur. In the center case of common asymmetry, the lowest vibrational level (localized in the right-hand-side well) gives rise to strong O^0 and weak T_0^1 lines. In the right-hand-side case of reversed asymmetry, the lowest vibrational level gives rise to weak O_0^0 and strong T_0^1 lines. In both asymmetric cases, other transitions originate in the higher well.

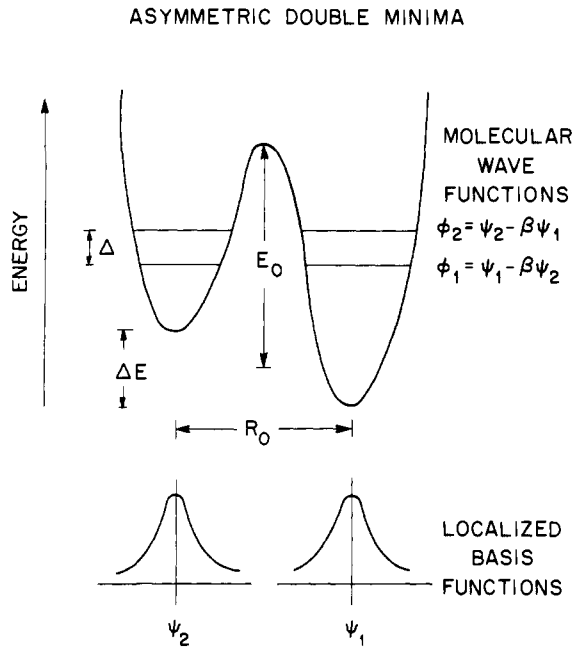

Figure 2. Schematic diagram of parameters appearing in the characterization of a slightly asymmetric double-minimum potential.

havior in argon host we determined $\Delta(d) = 9 \pm 1$ cm^{-1}.. In **1**-*h*, $\Delta(h)$ is too large for O^- to be thermally populated in solid Ne or Ar. However, from an analysis of the potential shape based upon **1**-*d* data, we estimated $\Delta(h) \simeq 130$ cm^{-1}.

In **1**-*d*, the spectral splitting between $O^+ \rightarrow O^+$ and $O^- \rightarrow O^-$ allowed us to determine that $\Delta^*(d) = 170$ cm^{-1} in the excited state. Both $\Delta^*(h)$ and $\Delta^*(d)$ are much larger than in the ground state, showing that the excited state tunneling barrier E_0^* is small. In the excited state, both $O^-(h)$ and $O^-(d)$ lie far too high to be thermally populated in fluorescence.

How will these phenomena change as a slight asymmetry is introduced into the potential? Asymmetry tends to localize the molecular eigenfunctions (eq 1) as outlined in Figure 2. In general, localization will be significant when one well is preferentially stabilized by an amount ΔE of the order of the tunneling splitting Δ in the symmetric parent **1**. Thus we expect a small asymmetry of only $\Delta E \sim 10$ cm^{-1} will significantly localize the ground state of **1**-*d*. An asymmetry of $\Delta E \sim 150$ cm^{-1} will

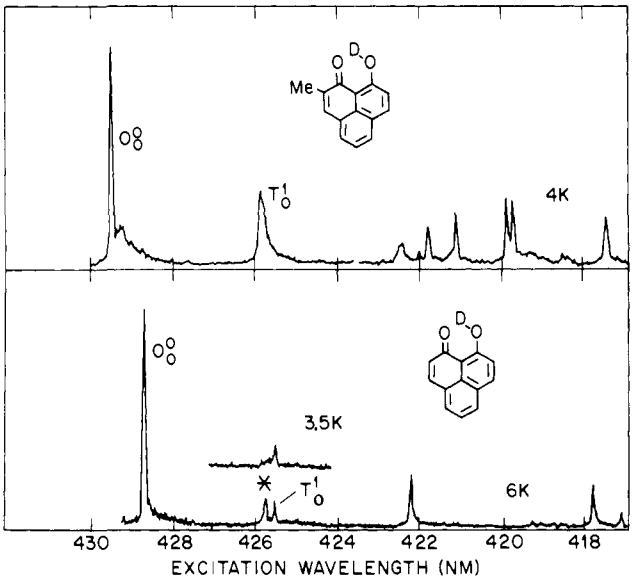

Figure 3. Comparison of the excitation spectrum of **2**-*d* with that of **1**-*d* reported in ref 1. Vibronic assignments as discussed in the text.

significantly localize the ground state of **1**-*h* and the excited state of **1**-*d*.

There are two major spectroscopic consequences as the wave functions begin to localize: (a) the splitting Δ will increase from its value in **1**, and (b) tunneling transitions which are forbidden in **1** should become allowed. (If this happens, Δ no longer gives the tunneling time via the Uncertainty Principle.) For example, if O^+ begins to localize in the ground electronic state, then "$O^+ \rightarrow O^-$" should become allowed. We label this line T_0^1 in the middle schematic of Figure 1. This middle schematic is applicable to the common asymmetry case where the same well is stabilized in both electronic states. The T_0^1 label implies a vibronic transition to the first excited vibrational state of the tunneling mode. The strength of $O_0^0(O^+ \rightarrow O^+)$ relative to T_0^1 will depend upon the degree of localization in excited and ground states. In the fluorescence, the T_1^0 line will appear if either the excited or ground state wave function is partially localized.

It is relatively simple to work out the asymmetric potential shape from the tunneling mode spectroscopic data. The experimental difficulty lies in the fact that these lines are embedded in many other vibronic lines reflecting geometry changes along other normal modes. In order to separate these T_0^1 lines from other vibronic lines, the normal procedure would be to compare the spectra of the *h* and *d* species. In the present case, this comparison is unusually complicated because we have discovered in symmetric **1**, and in the similar case of tropolone,[7] that deuteration actually changes the equilibrium structure of the molecule, in addition to changing the vibrational energy levels of the tunneling mode. This failure of the Born–Oppenheimer separation appears to occur because the π-electron distribution is sensitive to the fraction of time the tunneling nucleus spends inside the classically forbidden barrier. This fraction is reduced in the deuteride, leading to a different π-electron distribution and equilibrium geometry.

These complications imply that interpretation of the spectra is not straightforward. We will present a plausible, self-consistent interpretation for **2** in this paper; the reader will recognize that our discussion is more speculative and subjective than is normally the case in the electronic spectroscopy of smaller and simpler molecules.

The key to our interpretation lies in the comparison of the excitation spectra in **1**-*d* and **2**-*d* in Figure 3. We now offer an interpretation for **1**-*d* beyond that advanced in I. In solid neon, we found that the thermally populated $O^- \rightarrow O^-$ lies 160 cm^{-1} blue of $O^+ \rightarrow O^+$. This value, when combined with the ground state $\Delta(d)$ of about 10 cm^{-1}, predicts that the C_{2v} forbidden $O^- \rightarrow O^+$

(7) R. Rossetti and L. E. Brus, *J. Chem. Phys.*, 73, 1546 (1980).

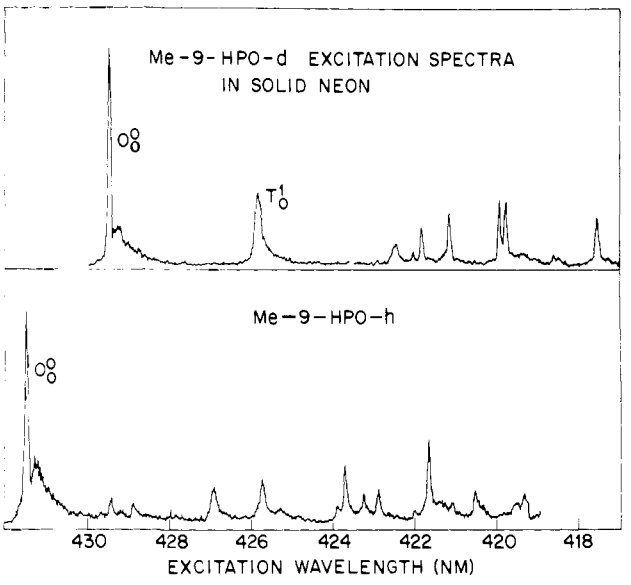

Figure 4. Normalized excitation spectra of **2**-*d* and **2**-*h* in solid neon.

(or T_0^1) line would occur about 170 cm^{-1} blue of $O^+ \rightarrow O^+$ (or O_0^0). There is actually a weak (~tenfold decrease) band present here as seen in Figure 3. We now believe that this band is the "forbidden" $O^- \rightarrow O^+$ (T_0^1) present because of static environmental perturbation.

The ground state of **1**-*d* has the smallest tunneling splitting $\Delta(d) \simeq 10$ cm^{-1}. This state will be the first state to localize as a result of an asymmetric environment, because it has the smallest matrix element establishing delocalization in the absence of perturbation. If the local neon environment stabilizes the potential well on one oxygen by just several cm^{-1} more that the other well, then the eigenfunctions will partially localize. Previous experience with neon matrix isolation of moderately high symmetry molecules has shown that the small matrix static perturbation is of low symmetry. The net effect is that vibronic lines forbidden in the isolated molecule group become very weakly allowed, due to host-induced mixing of nearby states. This effect has been observed among the fine structure components of the $^1\Delta + {}^1\Delta$ state of $(O_2)_2$ dimer,[8] the two degenerate $n-\pi^*$ triplets of *p*-benzoquinone,[9] and the "resonating" $^1B_{2u}$ and $^1B_{3g}$ states of biphenyl.[10] In view of these studies, our assignment of this line of **1**-*d* as T_0^1 is plausible.

In contrast to the symmetric **1**-*d* result, there is no temperature-dependent $O^- \rightarrow O^-$ feature in **2**-*d* in either neon or argon matrices. We conclude that methyl substitution has stabilized one well, and therefore increased $\Delta(d)$, such that the O^- level is no longer thermally accessible. In **1**-*d* we found $\Delta(d) = 9 \pm 1$ cm^{-1}, and we conclude that $\Delta(d) \geq 40$ cm^{-1} in **2**-*d*. Model calculations, to be described in the Theory section, show that the ground vibrational state (of the ground electronic state) must be completely localized in **2**-*d*. The molecular eigenfunctions are ψ_1 and ψ_2 and not $\phi^{\pm}$.

If the ground state of **2**-*d* is completely localized, then the T_0^1 band should be present without external perturbation. In Figure 3 it appears that the T_0^1 line has substantially intensified and slightly shifted blue from 172 cm^{-1} to 197 cm^{-1} above 0_0^0 in **2**-*d*. This strong transition in **2**-*d* does not appear at this energy in **2**-*h*, as must be the case for T_0^1, as seen in Figure 4. $\Delta^*(d)$ increases from 170 cm^{-1} in **1**-*d* to 197 cm^{-1} in **2**-*d*. This small percentage increase implies that the **2**-*d* excited electronic state vibrational wave functions are still significantly delocalized, in contrast to the ground electronic state. The fact that T_0^1 is strong in **2**-*d* also is consistent with localized ground state wave functions and significantly delocalized excited state wave functions. In the Theory section, the increase of $\Delta^*(d)$ from **1**-*d* to **2**-*d* is used to derive the excited state asymmetry ΔE^* in Figure 2 due to methyl substitution.

If T_0^1 is strong in absorption, then T_1^0 must also be present in emission. Identification of T_1^0 proved to be difficult. In absorption, identification of T_0^1 in **2**-*d* is possible as the spectrum is relatively simple. In emission, however, there are many vibronic lines as seen in Figure 5, and the spectral changes from **1** are significant.

In both **2**-*d* and **2**-*h*, extensive experiment shows that there is one "unique" vibronic feature as judged by its behavior (a) across the inhomogeneous line shape and (b) upon going from neon to argon host. Polyatomic molecules in matrices invariably occur in several well-defined sites energetically spread over ~10–20 cm^{-1} in the electronic spectrum. The spectrum of one site can be obtained by exciting just that site with a spectrally narrow tunable laser. Each site represents the molecule with a different arrangement of matrix atoms around it. Normally molecular vibrational frequencies and Franck–Condon factors are independent of site. This simply reflects the fact that molecular vibrations are controlled by chemical valence forces on nuclei, and are weakly sensitive to external van der Waals interactions when the amplitude of vibration is small.

Figure 5 shows bands labelled T_1^0 for **2**-*h* and **2**-*d*. These bands shifted in separation from O_0^0, and varied in relative Franck–Condon factor with respect to O_0^0, as different sites were excited, in contrast to all other major vibronic bands in both isotopes. Figure 6 shows this effect in **2**-*h* as a function of excitation wavelength. The Franck–Condon factor varies by ~2×, and the shift from 159 to 179 cm^{-1}, in these three spectra. In order to determine whether T_0^1 is really emission in isolated molecules of **2**, and not fluorescence of an impurity or **2** complexed with an impurity, we took excitation spectra while monitoring T_0^1 emission as well as while monitoring normal vibronic bands such as A and C in Figure 5. All these spectra showed the same excited state structure characteristic of **2**. There is no doubt that T_1^0 as well as normal bands like A and C originate in the same isolated molecules.

The uniqueness of these lines with respect to environment is naturally explained if these lines are the expected T_1^0 tunneling vibronic bands. The T_1^0 transition moves a nucleus partially localized in well **1** to a state almost completely localized in well **2**. In this transition the proton should sense the existence of host atoms around both wells as well as in the barrier region between. This unusually large amplitude motion should be especially sensitive to the structure of environment.

Another factor favoring the assignment of the T_1^0 line to the tunneling vibronic transition involves the strength of this transition in **2**-*h*. In Figure 5, T_1^0 is in fact the strongest vibronic band. It is stronger than the A and C bands which we shall assign as analogous to the dominating A and C bands of **1**-*h*. The appearance of an intense, low-frequency vibronic band in asymmetric **2** is naturally explained as T_1^0; it is hard to imagine how methylation could otherwise cause the appearance of this intense feature with isotope specificity.

O_0^0 is stronger than T_1^0 and T_0^1 in both isotopes. Inspection of Figure 1 shows that, within the Franck–Condon principle, this can only occur if **2** corresponds to common asymmetry and not reverse asymmetry. **2** is thus different than the previously discussed cases of **4**, **5**, and **6**.

B. Other Vibronic Structure. If we compare the fluorescence vibronic structure of **2** with that of **1** we find that Franck–Condon factors are generally smaller in **2**. In **1** there were two dominant modes A and C whose 284 cm^{-1} and 625 cm^{-1} frequencies were indepenent of deuteration. In **2**, A and C appear to correspond to lines at 331 cm^{-1} and 549 cm^{-1}. The decrease in C frequency in **2** is reasonable for an in-plane ring distortion moving the substituted carbon; methylation would effectively increase this carbon's mass.

In **1** we found A to be anomalous in that its Franck–Condon factor increased upon deuteration, while its frequency was independent of deuteration. We suggested that A represented a mode

(8) J. Goodman and L. E. Brus, *J. Chem. Phys.*, **67**, 4398 (1977).
(9) J. Goodman and L. E. Brus, *J. Chem. Phys.*, **69**, 1604 (1978).
(10) A. Baca, R. Rossetti, and L. E. Brus, *J. Chem. Phys.*, **70**, 5575 (1979).
(11) C. Svensson, S. C. Abrahams, J. L. Bernstein, and R. C. Haddon, *J. Am. Chem. Soc.*, **101**, 5759 (1979).

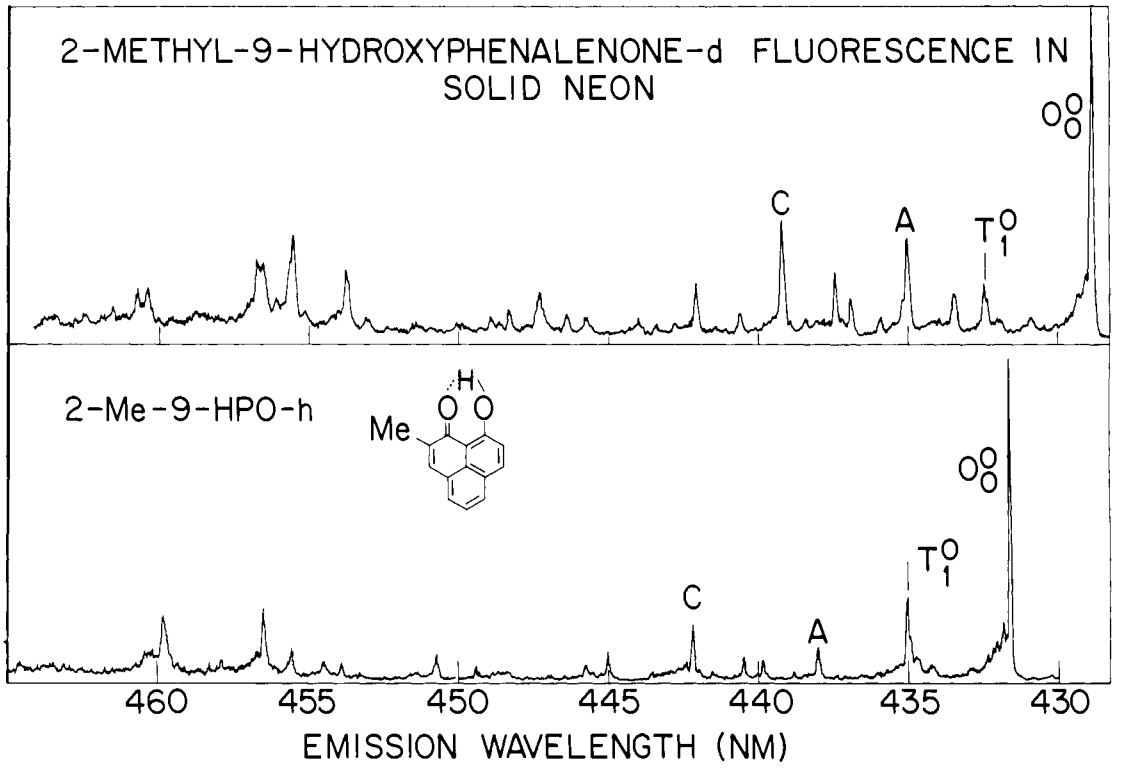

Figure 5. Emission spectra of **2-*d*** and **2-*h*** in solid neon. The resolution is about 0.1 nm.

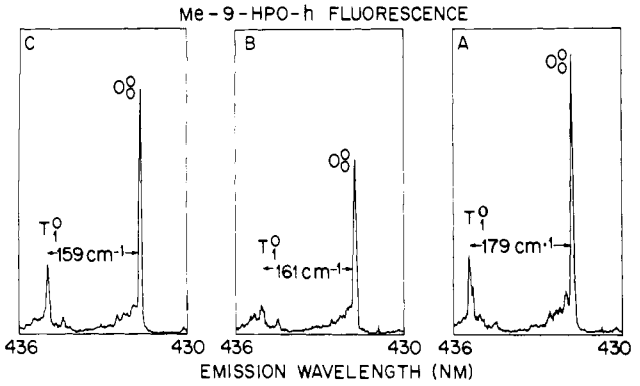

Figure 6. Variation in the emission spectra of **2-*h*** with excitation wavelength. The Franck–Condon factor and vibrational splitting of T_1^0 change as different sites are excited within the inhomogeneous line width. The excitation spectral shift between A and B, and B and C, is +3 cm^{-1}.

whose equilibrium position in the excited state was sensitive to the time-averaged position of the tunneling nucleus. For example, a chelate ring bend modulating the O···O distance might be sensitive to the time the tunneling mass spent inside the barrier region. In **2** we see now that A is further anomalous in that methylation appears to increase the ground state frequency from 284 cm^{-1} to 331 cm^{-1}. This does not appear to be a reduced mass effect. It may be that localization of the vibrational wave function in one well affected the ground state π-electron distribution and increased the force constant of this mode.

In I we remarked that the excitation spectrum of **1-*d*** was very different than that of **1-*h***. The excited state structure is strongly dependent upon tunneling mass as the **1-*h*** energy level is near the top of the tunneling barrier E_0^*. Figure 4 shows these same remarks apply to **2**. The emission and excitation spectra are tabulated in Tables I and II.

C. Comparison of Neon and Argon Hosts. As is usually the case, almost all of the vibrational frequencies appearing in the excitation and emission spectra are essentially independent of host. The T_1^0 lines provide the exception. In argon host these lines were generally weaker than they are in Figure 5, and for some sites appeared to be entirely absent. When present, the T_1^0 frequencies were somewhat smaller. An asymmetric packing of Ar atoms around the asymmetric **2** strongly affects the tunneling process, as suggested for Ne previously.

Table I. Excitation Spectrum Vibronic Structure in Solid Neon

2-*h*			2-*d*		
I	*E*, cm^{-1}	ΔE, cm^{-1}	*I*	*E*, cm^{-1}	ΔE, cm^{-1}
8.5	23 165		7.5	23 275	
0.8	23 403	238	2.5	23 472	197(T_0^1)
1.0	23 492	327	0.6	23 661	386
1.6	23 590	425	1.2	29 696	421
0.5	23 621	456	1.6	23 736	461
0.8	23 643	478	2.2	23 805	530
2.3	23 720	555	2.2	23 815	540
0.6	23 795	630	1.5	23 941	666

Table II. Emission Vibronic Structure for **2-*h*** and **2-*d*** in Solid Neon

2-*h*			2-*d*			comments
I	*E*, cm^{-1}	ΔE, cm^{-1}	*I*	*E*, cm^{-1}	ΔE, cm^{-1}	
8.5	23 165		9.3	23 275		O_0^0
~2.3		159-178	~1.2		169-193	T_0^1
			1.0	23 028	247	
0.9	22 831	334	2.5	22 944	331	"A"
0.5	22 735	430	0.8	22 846	429	
0.5	22 701	464	1.5	22 818	457	
1.5	22 616	550	2.8	22 726	549	"C"
0.7	22 470	695	0.5	22 656	619	
0.3	22 433	732	1.2	22 599	695	
0.3	22 252	913				
0.7	22 186	979	1.0	22 316	958	
0.4	22 033	1133				
0.4	22 002	1163				
0.9	21 976	1190	1.6	22 002	1273	
1.8	21 906	1260	2.2	21 917	1358	
1.6	21 749	1417	1.5	21 864	1411	

Theory

Tunneling in a molecule the size of **2** is a complex multidimensional dynamical process. In order to develop a physical picture, using our limited experimental data, we employ a simple

Table III. Asymmetric Double-Minimum Parameters for 2-Methyl-9-hydroxyphenalenone as Defined in Figure 2[a]

parameter	ground state	excited state
E_0, cm^{-1}	4950	1470
R_0, Å	0.48	0.42
ΔE, cm^{-1}	180	120
$\Delta(h)$, cm^{-1}	~199	~577
$\beta^2(h)$	0.05	0.64
$\Delta(d)$, cm^{-1}	~180	197
$\beta^2(d)$	0.004	0.29

[a] E_0 and R_0 are taken from the best fits to 1 described in ref 1. ΔE, Δ, and β^2 are derived from our data as described in the text.

model with a tunneling coordinate R representing the O···H···O proton motion. The potential can be represented as

$$V(R) = A(R^4 - BR^2) + CR \qquad (2)$$

yielding the characteristic Figure 2 shape. The linear term (CR) preferentially stabilizes one well, and shifts the equilibrium position with respect to symmetric **1**. In the case of **1** where C and ΔE are zero, we had to make two further assumptions in order to characterize the potential from the datum $\Delta(d)$.

First, the reduced tunneling mass is that of a free proton or deuteron. This is not necessarily true as, within the one-dimensional model, the fact that C and O nuclei also move as the molecule tunnels from one cannonical structure to the other might be taken into account by using a somewhat heavier reduced mass. However, in a recent study of similar processes in tropolone, it was experimentally found that the tunneling masses are within 10% of the free proton (deuteron) masses.[7] Therefore, this approximation is probably not severe in **1** and **2**.

Second, the value of R_0 is taken to be near $R_0 \simeq 0.4$ Å as suggested by an X-ray structural study.[10] We found that the calculated value of $\Delta(h)$ is relatively insensitive to the exact value of R_0 near 0.4 Å, but that the barrier height E_0 is quite sensitive. Representative parameters for ground and excited states appear in Table III.

In analyzing our data for **2**, we vary C while holding A and B fixed at the values obtained in **1**. Eigenfunctions and energy levels are determined, using the variational theorem, by minimizing

$$\langle E_1 \rangle = \frac{\int \phi_1 \hat{H} \phi_1 \, dR}{\int \phi_1 \phi_1 \, dR} \qquad (3)$$

where the two lowest vibrational wave functions are

$$\phi_1 = \psi_1 + \beta\psi_2 \qquad \phi_2 = \psi_2 - \beta\psi_1 \qquad (4)$$

ψ_1 and ψ_2 are Gaussian wave functions $\exp[-\alpha(\Delta R)^2]$localized in wells **1** and **2** as shown in Figure 2. Note that β is dependent upon isotopic substitution.

In the case of **1**, $C = 0$ and $\beta = 1$. Here ϕ_1 and ϕ_2 become $\phi^{\pm}$, and α is chosen to closely reproduce the splittings $\Delta(h)$ and $\Delta(d)$ determined previously for **1**. This value of α is then used for **2**, and we find $\Delta(h)$ and $\Delta(d)$ for **2** by minimizing $\langle E \rangle$ as a function of β for each assumed C.

The excited state of **2**-*d* is characterized by $\Delta^*(d) = 197$ cm^{-1} as compared with $\Delta^*(d) = 172$ cm^{-1} for **1**-*d*. Our calculation reproduces this 25 cm^{-1} increase for a value of C corresponding to $\Delta E^* = 120$ cm^{-1}. As seen in Table III, ϕ_1 is still substantially delocalized with $\beta^2(h) = 0.64$ and $\beta^2(d) = 0.30$.

In the ground electronic state of **2**, there is a substantial site and host dependence to $\Delta(h)$ and $\Delta(d)$. Nevertheless, for a rough estimate we take $\Delta(d) \simeq 170$ cm^{-1} and find $\Delta E \simeq 180$ cm^{-1} and $\Delta(h) \simeq 199$ cm^{-1}. In the ground state ϕ_1 is essentially localized in both **2**-*d* and **2**-*h*, with $\beta^2(h) = 0.05$ and $\beta^2(d) = 0.004$. The asymmetric potentials in both excited and ground electronic states appear in Figure 7.

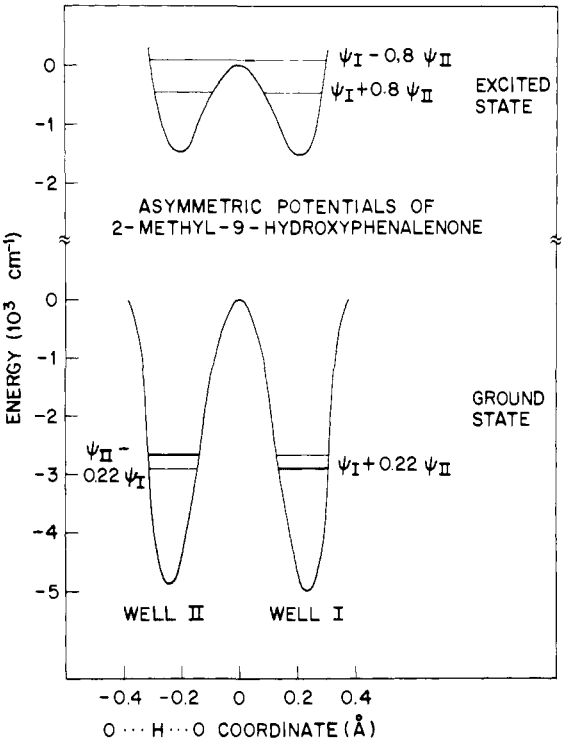

Figure 7. The derived asymmetric potentials for **2**-*h*. As discussed in the text and parameterized in Table III, the asymmetry is barely perceptible when compared with the barrier height E_0 present in the symmetric parent **1**. For each vibronic state, the calculated eq 4 wave functions are shown. The zero-order symmetric potentials are the $R_0 = 0.48$ Å and $R_0^* = 0.42$ Å cases discussed in ref 1.

Conclusions

(1) Methyl substitution in the 2 position stabilizes one local minimum by a relatively small amount: $\Delta E \simeq 180$ cm^{-1} in the ground electronic state, and $\Delta E^* \simeq 120$ cm^{-1} in the excited state. The same well is stabilized in both electronic states. This stabilization localizes the vibrational wave function in the ground electronic state; however, the excited state is substantially delocalized as the tunneling barrier E_0^* is small. In the ground state, the stabilization ΔE is only ~0.04 times the size of E_0, and a second well-defined local minimum still exists on the other oxygen.

(2) The extreme sensitivity of the electronic spectrum to phenolic deuteration, and the small shift in the electronic state energy with substitution in **2** suggest that the π–π^* electronic state has a large amplitude on the tunneling chelate ring.

(3) Intramolecular tunneling splittings in the range 10–10^2 cm^{-1} are sensitive to asymmetric host perturbation, even in solid neon host, in contrast to normal molecular vibrations. This sensitivity apparently reflects the large amplitude of motion and delicate balance of forces in the tunneling process.

(4) The anomalous behavior of the A vibration, and the dependence of equilibrium geometry upon deuteration, suggest that the π-electron structure is correlated with the time-averaged position of the tunneling nucleus.

Acknowledgment. We thank F. H. Stillinger for stimulating discussions of tunneling dynamics.